

Commed Copy

5

PLASMA PHYSICS LABORATORY
THE COLLEGE OF WILLIAM AND MARY IN VIRGINIA
Williamsburg, Virginia

N66-15979

FACILITY FORM 802

(ACCESSION NUMBER)	(THRU)
54	1
(PAGES)	(CODE)
CL 69655	25
(NASA CR OR TMX OR AD NUMBER)	(CATEGORY)

GPO PRICE \$ _____

CFSTI PRICE(S) \$ _____

Hard copy (HC) 3.00

Microfiche (MF) .50

653 July 65

BIMCDAL-CAVITY MEASUREMENT OF THE MICROWAVE FARADAY
EFFECT IN A GASEOUS MAGNETOPLASMA

by M. T. Raiford

Technical Report No. 2, ~~Aug. 1963~~
June 1963

NASA RESEARCH GRANT NSG 106-61

This work was submitted to the College of William and Mary in Virginia as a thesis in partial fulfillment of the requirements for the degree of Master of Arts in Physics, June, 1963.

The work was supported by the National Aeronautics and Space Administration under Research Grant NSG 106-61.

Approved: _____

Frederic R. Crownfield, Jr.
Frederic R. Crownfield, Jr.
Principal Investigator

ACKNOWLEDGMENTS

The author would like to thank Professor Frederic R. Crownfield, Jr., under whom this work was done, for his help and guidance throughout this investigation. Thanks also go to the faculty and staff of the Physics Department for their help and advice, and especially to Professor James D. Lawrence, Jr., and Professor Louie A. Galloway for their reading and criticism of the manuscript. This investigation was supported by the National Aeronautics and Space Administration under research grant number NSG 106-61.

TABLE OF CONTENTS

	Page
ACKNOWLEDGMENTS	11
LIST OF FIGURES	1v
ABSTRACT.	v
I. INTRODUCTION AND BACKGROUND	2
II. THE BIMODAL CAVITY CONTAINING A COMPLEX MEDIUM.	10
III. EQUIPMENT	
A. EXPERIMENTAL ARRANGEMENT.	21
B. THE MAGNET.	23
C. THE CAVITY.	26
D. DISCHARGE APPARATUS	28
IV. PROCEDURE AND DATA.	30
V. EXPERIMENTAL RESULTS AND CONCLUSIONS.	38
VI. SUMMARY	41
BIBLIOGRAPHY.	43

LIST OF FIGURES

Figure	Page
1. Theoretical Curves of Power Output as a Function of Magnetic Field for Various Collision Frequencies	20
2. Block Diagram of Experimental Apparatus	22
3. Photograph of Air-core Magnet and Cavity.	24
4. The Magnet.	25
5. Diagram of the Microwave Cavity	27
6. Output Power vs. Magnetic Field; discharge current as a parameter Neon at 7.5 mm. pressure.	32
7a. Output Power vs. Magnetic Field. Neon, 4 mm. pressure.	34
7b. Output Power vs. Magnetic Field. Neon, 10 mm. pressure	35
7c. Output Power vs. Magnetic Field. Neon, 1 mm. pressure.	36

ABSTRACT

15979

Faraday Rotation of microwaves in a magnetized plasma has been observed using a microwave cavity technique. The positive column of a gaseous discharge was placed coaxially within a cylindrical cavity, with a magnetic field applied along this same axis. The cavity was excited in the angularly dependent TE_{111} mode, which is doubly degenerate, at a frequency in the neighborhood of 2000 MC. An input antenna was coupled to one of the degenerate modes and an orthogonal output antenna coupled to the other. Theory shows that the power coupled to the output is proportional to the absolute square of the off-diagonal element of the conductivity tensor of the anisotropic plasma. This gives a curve of output power as a function of magnetic field which is strongly dependent on collision frequency and also dependent on electron density.

The cavity was tuned up so that for zero magnetic field, there was no power transmitted to the output. Deviations from this null were recorded as the magnetic field was swept from zero to its maximum value, the signal frequency being kept constant. The recorded power coupled to the output gave resonance curves in agreement with the theoretical predictions.

Author

**BIMODAL-CAVITY MEASUREMENT OF THE MICROWAVE FARADAY
EFFECT IN A GASEOUS MAGNETOPLASMA**

I. INTRODUCTION AND BACKGROUND

In 1845, Faraday discovered that when a beam of linearly polarized light was passed through a transparent medium immersed in a magnetic field, the plane of polarization was rotated through an angle which was directly proportional to the strength of the field and the length of the medium traversed.¹ This is known as the Faraday Effect, and the angle of rotation is usually written as $\theta = V B_0 L$, where V is the Verdet constant of the medium, B_0 the magnetic induction, and L the length of the medium. This effect was explained much later in terms of the Fresnel decomposition of a linear wave into two oppositely rotating circularly polarized waves.

In recent years, there has been a great deal of interest in the Faraday Effect for microwaves in ferrites^{2,3} and for gaseous plasmas.²⁻⁵

¹F. A. Jenkins and H. E. White, Fundamentals of Optics, (McGraw-Hill Book Co., Inc., New York, 1957). p. 596

²H. Suhl and L. R. Walker, Bell Telephone Laboratory Monograph No. 2322, 1954.

³L. Goldstein, M. Gilden, and J. Etter, IRE Convention Record, Part 10, p. 58, 1953.

⁴L. Goldstein, Advances in Electronics and Electron Physics, Ed. L. Marton, (Academic Press, New York), Vol. VII. p. 483, 1955.

⁵J. E. Etter and L. Goldstein, U. of Illinois E. E. Res. Tech. Rept. No. 3, Contract No. AF 19(604)-525, p. 42, 1954. (ASTIA No. AD 53596).

In ferrites, it is a magnetic effect in that the electron spins give rise to a permeability tensor, while in plasmas it is an electric effect since the medium is characterized by a tensor dielectric coefficient. In this work, we shall be interested only in the latter case.

Propagation of guided microwaves through plasmas in a magnetic field was first reported by Goldstein, Lampert, and Heney⁶ in 1951. They observed large Faraday Rotations, and, in addition a resonance effect where the cyclotron frequency of the electrons equals the microwave signal frequency, polarization transformations, and non-reciprocity of propagation. The explanation of the effect in plasmas is that the applied static magnetic field renders the medium anisotropic, so that the plasma is characterized by a dielectric coefficient in the form of a tensor. The derivation using Maxwell's equation and the equation of motion of the electrons in the plasma is given by Ginzburg.⁷ When the static magnetic field B_0 is taken along the Z-direction, the dielectric tensor is:

$$\epsilon = \begin{bmatrix} \epsilon_1 & -i\eta & 0 \\ i\eta & \epsilon_1 & 0 \\ 0 & 0 & \epsilon_2 \end{bmatrix} \quad (1)$$

⁶L. Goldstein, M. Lampert, and J. Heney, Phys. Rev. 82, 956, (1951).

⁷V. L. Ginzburg, Propagation of Electromagnetic Waves in Plasma, (Gordon and Breach Science Publishers, Inc., New York, 1961) p. 158.

where

$$\epsilon_1 = \epsilon_0 \left[1 + \frac{\frac{\omega_p^2}{\omega^2} (1 - i \frac{\nu}{\omega})}{\frac{\omega_c^2}{\omega^2} - (1 - i \frac{\nu}{\omega})^2} \right], \quad (2)$$

$$\eta = \epsilon_0 \left[\frac{\frac{\omega_c^2}{\omega^2} - \frac{\omega_p^2}{\omega^2}}{\frac{\omega_c^2}{\omega^2} - (1 - i \frac{\nu}{\omega})^2} \right], \quad (3)$$

and

$$\epsilon_2 = \epsilon_0 \left[1 - \frac{\frac{\omega_p^2}{\omega^2}}{1 - i \frac{\nu}{\omega}} \right] \quad (4)$$

In the expressions above, ω is the microwave signal frequency, ν is the effective collision frequency for the electrons, ω_p is the angular plasma frequency, given by

$$\omega_p^2 = \frac{Ne^2}{\epsilon_0 m}, \quad (5)$$

and ω_c is the electron cyclotron frequency given by

$$\omega_c = \frac{e B_0}{m} \quad (6)$$

Here

N = electron density of the plasma

e = electron charge

m = electron mass

ϵ_0 = permittivity of free space

This tensor is the starting point for discussions of Faraday Rotation. A basic understanding of the effect is afforded by considering the case of uniform plane waves propagating in an unbounded medium. Etter and Goldstein⁸ give a good general discussion, the results of which are outlined below:

Assuming plane wave solutions of the form $e^{i\omega t - \gamma z}$ to Maxwell's equations, one obtains for the propagation constant

$$\gamma_{\pm}^2 = -\omega^2 \mu_0 (\epsilon_1 \pm \eta) \quad (7)$$

where $\gamma = \alpha + i\beta$, α being the attenuation constant and β the phase constant. μ_0 is the permeability of free space, and ϵ_1 and η are components of the dielectric tensor given above. One also obtains a relationship between the field components of

$$\left(\frac{E_x}{E_y} \right)_{\pm} = \pm i \quad (8)$$

which correspond to oppositely rotating circular waves, the (+) referring to one of the waves and the (-) to the other.

⁸ J. E. Etter and L. Goldstein, U. of Illinois E. E. Res. Lab. Tech. Rept. No. 3, 1954.

If the two waves are excited with equal amplitudes, the result is a plane polarized wave at the transmitter. If α is negligible, the resulting wave after traversing a distance L is also plane polarized but with its plane of polarization rotated through an angle θ given by

$$\theta = \frac{\beta_+ - \beta_-}{2} L, \quad (9)$$

where β_{\pm} are the two phase constants. If one assumes small fields and small electron densities, and compares this expression to the classical one of $\theta = V B_0 L$, the Verdet constant of the plasma is

$$V = \frac{|e^3| N}{2 m^2 \omega^2} \sqrt{\frac{\mu_0}{\epsilon_0}} \quad (10)$$

Therefore, in this limit, rotation is directly proportional to magnetic field. If, however, the field is not restricted to small values and the electron cyclotron frequency ω_c is allowed to reach the value of ω , a resonance occurs in the expression for θ above. While for optical frequencies such a condition is not attainable, a field of $0.1 \frac{W}{M^2}$ makes $\omega_c = 2800$ Mc. Typical rotation curves showing anomalous behavior at cyclotron resonance ($\omega = \omega_c$) are given by Goldstein, et al.^{9, 10}

In the above work and in practically all work on Faraday Rotation up to the present, the propagation method has been used.

⁹ L. Goldstein, M. Gilden, and J. Etter, IRE Convention Record, Part 10, p. 62, 1953.

¹⁰ K. Rae and L. Goldstein, U. of Illinois E.E. Res. Sci. Rept. No. 3, Contract No. AF 19(604)-3481, p. 26, 58, 1962.

A typical experiment^{11,12} consists in propagating microwaves through a wave guide in which a discharge tube has been placed. This section of the microwave circuit is placed on the axis of a solenoid, and the actual angle of rotation, as well as polarization transformations, are measured as a function of magnetic field. The microwave analog of a linear light wave, in this case the TE_{11} mode in a circular wave guide, is used. Actually, in the presence of a magnetized plasma, one no longer has a pure TE_{11} wave, but in the limit as the magnetic field goes to zero, it reduces to a pure mode.¹³ It is interesting to note that when the radial dimension of the plasma is small compared to that of the wave guide, the TE_{11} wave is essentially plane polarized in the plasma, and the above discussion of plane waves is a good approximation.¹⁴

¹¹K. Rao and L. Goldstein, U. of Illinois E. E. Res. Sci. Rept. No. 3, Contract No. AF 19(604)-3481, p. 39, 1962.

¹²J. E. Etter and L. Goldstein, U. of Illinois E.E. Res. Tech. Rept. No. 3, Contract No. AF 19(604)-525, p.42, 1954. (ASTIA No. AD 53596.

¹³H. Suhl and L. R. Walker, Bell Telephone Monograph No. 2322, 1954.

¹⁴K. Rao and L. Goldstein, U. of Illinois E.E. Res. Sci. Rept. No. 3, Contract No. AF 19(604)-3481, p. 128, 1962.

In another facet of plasma research there has been considerable use of resonant microwave cavities to study basic plasma properties such as electron densities.¹⁵⁻¹⁷ These experiments utilize the fact that when a plasma is introduced into the cavity, the resonant frequency of a given mode shifts by a calculable amount. Buchsbaum, Mower, and Brown¹⁸ have worked out the frequency shifts for several lower order cylindrical cavity modes when a coaxial plasma-cavity system is placed in a magnetic field. In the case of degenerate modes, such as the $TE_{\lambda mn}$, the field has the effect of removing the degeneracy; the two degenerate modes undergo different frequency shifts.

One may combine the two areas of plasma investigations discussed above, and use microwave cavity techniques to study the Faraday Effect. This has been done in the case of ferrites by Portis and Teaney,¹⁹ who used a bimodal cavity to study electron spin resonance in paramagnetic materials. In the present work, the bimodal cavity has been used to study the Faraday Effect in a magnetized plasma. We will describe herein the cylindrical, coaxial plasma-cavity system used, both theoretically and experimentally.

¹⁵D. J. Rose and S. C. Brown, J. Appl. Phys. 23, 1026, (1952).

¹⁶M. A. Biondi, Rev. Sci. Inst. 22, 500, (1950).

¹⁷S. J. Buchsbaum, L. Mower, and S. C. Brown, Phys. Fluids 3, 1 (1960).

¹⁸Ibid.

¹⁹A. Portis and D. Teaney, J. Appl. Phys. 29, 1692 (1958).

When the empty cavity is excited in the TE_{111} mode, there exist two independent, orthogonal modes which may be resonant at the same frequency. A magnetoplasma is then introduced in the cavity which results in removal of the degeneracy and the introduction of coupling between the two otherwise independent modes. Faraday Rotation in this bimodal system is observed as a change in the coupling of the two modes.

II. THE BIMODAL CAVITY CONTAINING A COMPLEX MEDIUM

The theory of resonant cavities is well developed and has been known for a number of years. In 1950, Slater²⁰ published a complete account of the basic theory of the general resonant cavity. The approach is essentially the following: As is true of any vector field, the vector field in the cavity may be broken up into two fields, one being solenoidal (zero divergence), and the other irrotational (zero curl). The cavity fields may be expanded in terms of the normal modes of the cavity, which are orthogonal and may also be suitably normalized. The solenoidal fields are orthogonal to the irrotational ones. The current density may also be expanded in terms of these orthogonal functions, in a similar manner. After having thus obtained expressions for the electric field \bar{E} , the magnetic field \bar{H} , and the current density \bar{J} , these may be substituted into Maxwell's equations:

$$\bar{\nabla} \times \bar{E} = -\mu_0 \frac{\partial \bar{H}}{\partial t} \quad (11)$$

and

$$\bar{\nabla} \times \bar{H} = \epsilon_0 \frac{\partial \bar{E}}{\partial t} + \bar{J} \quad (12)$$

²⁰ J. C. Slater, Microwave Electronics, (D. Van Nostrand, Princeton, N. J., 1950), Ch. 4

In the above expression, \bar{J} is the polarization current density.

The curls in the above equations are expanded in terms of the orthogonal function in a manner similar to the above. This involves volume integrals over the cavity volume and some of these may be transformed into a surface integral by using a combination of vector identities and the divergence theorem. Substitution in the above equations leads to the following expression in terms of the expansion coefficients of the electric field modes:

$$\begin{aligned} \epsilon_0 \mu_0 \frac{d^2}{dt^2} \int \bar{E} \cdot \bar{E}_m dv + K_m^2 \int \bar{E} \cdot \bar{E}_m dv \\ = -\mu_0 \frac{d}{dt} \left[\int \bar{J} \cdot \bar{E}_m dv - \int_S (\hat{n} \times \bar{H}) \cdot \bar{E}_m da \right] \\ - K_m \int_S (\hat{n} \times \bar{E}) \cdot \bar{H}_m da \end{aligned} \quad (13)$$

In the above equation, \bar{E}_n and \bar{H}_n are the solenoidal functions used to expand their corresponding fields as described above; k_n is identified as the propagation constant of the n^{th} mode of these fields; and the integrals are over the cavity volume and surface. S' denotes the surface of any inputs and S denotes the remaining surface area of the cavity walls. This equation forms the basis of any further treatment of resonant cavities in general.

We now wish to extend the discussion to the case of a bimodal cavity in particular. Literature on this is rather sparse, although some discussion may be found in Berk and Lax²¹ and Portis and Teaney.²² The latter gave some theory based on an equivalent circuit of the resonant cavity system. Although there are several equivalent ways of looking at the problem, for our purposes the bimodal cavity seems to be most conveniently discussed in the following manner:

Starting with equation (13) above, we first note that this is just the differential equation describing the harmonic oscillator. The bimodal cavity operates in a mode, such as the TE_{111} , which is doubly degenerate, i.e., one that may oscillate, in the absence of a complex medium, in two independent, orthogonal modes. If the modes are not too strongly perturbed by the presence of the plasma, one may expand the electric field of such a cavity mode in terms of these two modes alone or

$$\bar{E} = \alpha \bar{E}_\alpha + \beta \bar{E}_\beta, \quad (14)$$

where \bar{E}_α and \bar{E}_β are the electric field components of each normal mode, and α and β are their corresponding amplitudes depending on the degree of excitation of each mode.

²¹A. D. Berk and B. Lax, IRE Convention Record, Part 10, p. 65, 1953. (See also p. 70).

²²A. Portis and D. Teaney, J. Appl. Phys. 29, 1692 (1958).

We are interested in a transmission-type bimodal cavity in which, with no magnetic field present, the input is coupled only to one mode, say the Q mode, and the output is coupled only to the L mode.

As mentioned previously, a magnetic field applied to a plasma renders it anisotropic, so that it is characterized by a dielectric tensor or a conductivity tensor. Thus the current density may be expressed in terms of the electric field as

$$\bar{J} = [\sigma] \bar{E}, \quad (15)$$

where the conductivity tensor $[\sigma]$ is obtained from the expression for the dielectric tensor given by equation (1) using the relation

$$[\sigma] = i\omega \left(\frac{[\epsilon]}{\epsilon_0} - [I] \right), \quad (16)$$

where $[I]$ is the unit tensor, Thus

$$\sigma = \begin{bmatrix} \sigma_1 & -i\sigma' & 0 \\ i\sigma' & \sigma_1 & 0 \\ 0 & 0 & \sigma_z \end{bmatrix}, \quad (17)$$

where

$$\epsilon_0 \sigma_1 = i\epsilon_0 \frac{\frac{\omega_p^2}{\omega} (1 - i\frac{\nu}{\omega})}{\frac{\omega_c^2}{\omega^2} - (1 - i\frac{\nu}{\omega})^2}, \quad (18)$$

$$\epsilon_0 \sigma' = i \epsilon_0 \frac{\frac{\omega_p^2}{\omega} \frac{\omega_c}{\omega}}{\frac{\omega_c^2}{\omega^2} - (1 - i \frac{\nu}{\omega})^2} \quad (19)$$

and

$$\epsilon_0 \sigma_z = -i \epsilon_0 \frac{\frac{\omega_p^2}{\omega}}{1 - i \frac{\nu}{\omega}} \quad (20)$$

Returning to equation (13), we now substitute equation (15) for \bar{J} , and equation (14) for \bar{E} . Using the orthonormality of the two modes, we have for $n = \alpha$

$$\begin{aligned} \epsilon_0 \mu_0 \frac{d^2}{dt^2} \alpha + k_\alpha^2 \alpha = -\mu_0 \frac{d}{dt} [\alpha(\eta)(\sigma_1) + \beta(\eta)(-i\sigma_1')] \\ + \mu_0 \frac{d}{dt} \int_{S_1'} (\hat{n} \times \bar{H}) \cdot \bar{E}_\alpha d\eta - K_\alpha \int_S (\hat{n} \times \bar{E}) \cdot \bar{H}_\alpha d\eta \end{aligned} \quad (21)$$

where C_1 is a constant depending on the geometry of the cavity and on the plasma volume, and S_1' corresponds to the surface of the input.

A similar expression is obtained for $n = \beta$:

$$\begin{aligned} \epsilon_0 \mu_0 \frac{d^2}{dt^2} \beta + k_\beta^2 \beta = -\mu_0 \frac{d}{dt} [\alpha(\eta)(i\sigma_1') + \beta(\eta)(\sigma_1)] \\ + \mu_0 \frac{d}{dt} \int_{S_2'} (\hat{n} \times \bar{H}) \cdot \bar{E}_\beta d\eta - K_\beta \int_S (\hat{n} \times \bar{E}) \cdot \bar{H}_\beta d\eta \end{aligned} \quad (22)$$

where S_2' corresponds to the surface of the output.

Also

$$k_m^2 = \omega_m^2 \mu_0 \epsilon_0, \quad k_m \vec{H}_m = \vec{\nabla} \times \vec{E}_m, \quad m = \alpha, \beta \quad (23)$$

Thus for a doubly degenerate mode there are two equations, one for each of the modes. The amplitudes of these satisfy harmonic oscillator equations. In addition, equations (21) and (22) are coupled, so that we have the standard problem of a pair of coupled harmonic oscillators, each oscillator representing one of the normal modes of the field.

The problem is then to find the power coupled to the output in terms of the known power driving the input. Since the output is connected to a passive load impedance of fixed value in our case, and we are interested only in the power reaching the output transmission line, one may regard the driving term of the output mode as effectively zero, lumping the termination in the properties of the modes. Then the equation governing the output mode may be regarded as having no driving force. The steady-state solution of these equations for a sinusoidal driving field then may be reduced in the standard way to the algebraic equations:

$$\begin{bmatrix} A_{11} & A_{12} \\ A_{21} & A_{22} \end{bmatrix} \begin{bmatrix} \alpha \\ \beta \end{bmatrix} = \begin{bmatrix} F \\ 0 \end{bmatrix} \quad (24)$$

where F is the driving force from the input on the α mode, and the A -matrix represents the coefficients of α and β . The off-diagonal components of the A -matrix are proportional to the corresponding components of the conductivity tensor, so that $A_{12} = -A_{21}$. Calling the determinant of this non-singular matrix D :

$$D = A_{11} A_{22} + A_{12}^2, \quad (25)$$

and solving equation (24) for β in terms of F , we have

$$\frac{\beta}{F} = \frac{A_{12}}{D} \quad (26)$$

This is proportional to the ratio of the amplitudes of the driving field to the output signal. Since we measure power, we desire an equation giving the output power in terms of the input power. This quantity is proportional to the absolute square of the above quantities, so that

$$\frac{P_{out}}{P_{in}} = \text{const} \frac{|A_{12}|^2}{|D|^2} \quad (27)$$

Now the determinant D is the same determinant occurring in the secular equation in the homogeneous case (no driving forces), from which it is known that a nontrivial solution exists if and only if the determinant vanishes. Its roots are the complex frequencies of the free modes of vibration. Thus the determinant may be written as a product of factors in these roots, times a constant.

For two modes, D is quadratic in ω , so

$$D(\omega) = G(\omega^2 - \omega_1^2)(\omega^2 - \omega_2^2) \quad (28)$$

where ω_1 and ω_2 are the complex resonant frequencies of the two normal modes of our cavity, corresponding to the α and β modes respectively, and G is some constant.

As described later, in the experiment the procedure is to tune the signal frequency ω to the frequency of the resonant modes (which have been made equal), but it is important to note here that ω is then equal to only the real parts of the complex frequencies of the cavity modes. Writing these complex frequencies as

$$\omega_1 = \omega_1' + i\omega_1'' \quad (29)$$

and

$$\omega_2 = \omega_2' + i\omega_2'' \quad (30)$$

where the imaginary parts are small compared to the real parts, and taking into account that in our case we have set $\omega = \omega_1' = \omega_2'$ equation (28) for D becomes

$$D = -4\omega^2 G(\omega_1''\omega_2'') \quad (31)$$

Now the imaginary parts of the frequencies are inversely proportional to the Q 's of the corresponding cavity modes. Buchsbaum et al²³ have derived expressions for the change in $1/Q$ for the degenerate TE_{111} mode, and the fractional change is small. In equation (31) the change in ω_1'' and ω_2'' is thus small, so that their product may be considered constant.

²³S. Buchsbaum, L. Mower, and S. C. Brown, Phys. Fluids 3, 1 (1960).

Thus we see that for a fixed signal frequency, the absolute square of D may be considered constant.

The absolute square of A_{12} is

$$|A_{12}|^2 = C_1^2 \epsilon_0^2 \frac{\omega_p^4}{\omega^2} \frac{\omega_c^2}{\omega^2} \frac{1}{\left(\frac{\omega_c^2}{\omega^2} - 1 + \frac{\gamma^2}{\omega^2}\right)^2 + 4 \frac{\gamma^2}{\omega^2}} \quad (32)$$

Lumping the constants in equations (27), (31), and (32) in K , we have finally,

$$\frac{P_{out}}{P_{in}} = K \omega_p^4 \left[\frac{\frac{\omega_c^2}{\omega^2}}{\left(\frac{\omega_c^2}{\omega^2} - 1 + \frac{\gamma^2}{\omega^2}\right)^2 + 4 \frac{\gamma^2}{\omega^2}} \right] \quad (33)$$

This is the desired result, showing explicitly the functional dependence of the power coupled to the output in terms of the parameters of the magnetized plasma.

It is seen that the result, equation (33), is a resonance-type expression. If one takes the derivative of this equation and equates it to zero, the maximum of this resonance curve is found to occur, not at $\omega_c = \omega$, but at

$$\omega_c^2 = \omega^2 + \gamma^2$$

(34)

It is also noted that the output power is proportional to the square of the electron density.

The theoretical curves obtained from equation (33) for a given signal frequency and plasma frequency are shown in Figure 1. The term in brackets (which depends on the field) is plotted against magnetic field strength for various collision frequencies. It is seen that the resulting curves are very sensitive to the collision frequency, the resonance peak occurring almost at $\omega_c = \omega$ for very low collision frequencies and being quite large and sharp. As the collision frequency increases, the peaks shift to the right (as expected from equation (34)) and become smeared out and smaller.

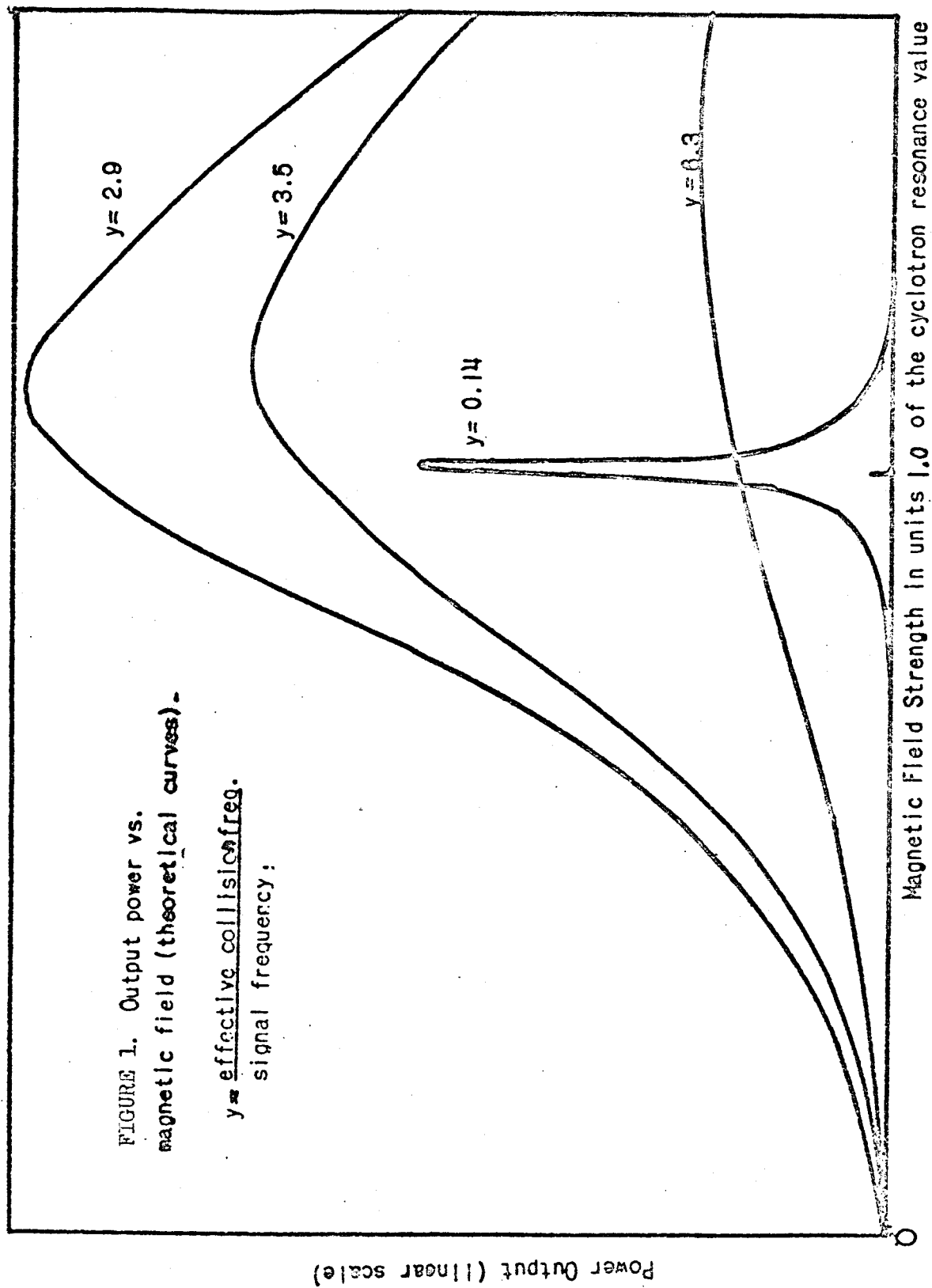


FIGURE 1. Output power vs. magnetic field (theoretical curves).

$y = \frac{\text{effective collision freq.}}{\text{signal frequency}}$

III. EQUIPMENT

A. Experimental Arrangement

A block diagram of the experimental arrangement is shown in Figure 2. As indicated in the figure, the cavity was driven by a Transition TS-403B/U signal generator (pulse) modulated at 1000 cycles. The input line was a coaxial cable connected to a BNC coaxial connector on the cavity; the connector was terminated by a short probe antenna. The output line was connected to a similar antenna at right angles to the input antenna, both of them located in the mid-plane of the cavity. The output signal was detected by a crystal detector mount* connected to the output antenna by means of a BNC connector. The resulting 1000 cycle signal was then amplified and detected by a Hewlett-Packard Model 415A SWR detector. This signal was then fed into the Y-input of a Moseley Model 135 X-Y Recorder. The X-input could either be operated by an internal, calibrated time sweep, or by an Empire Model 900 Hall-effect Gauss-meter. In the latter case the 3000 cycle signal from the output jack was rectified by a IN34A shunted across the recorder terminals.

*Part of Western Electric D-152393 (BO-20600) Standing Wave detector, modified to use BNC connectors.

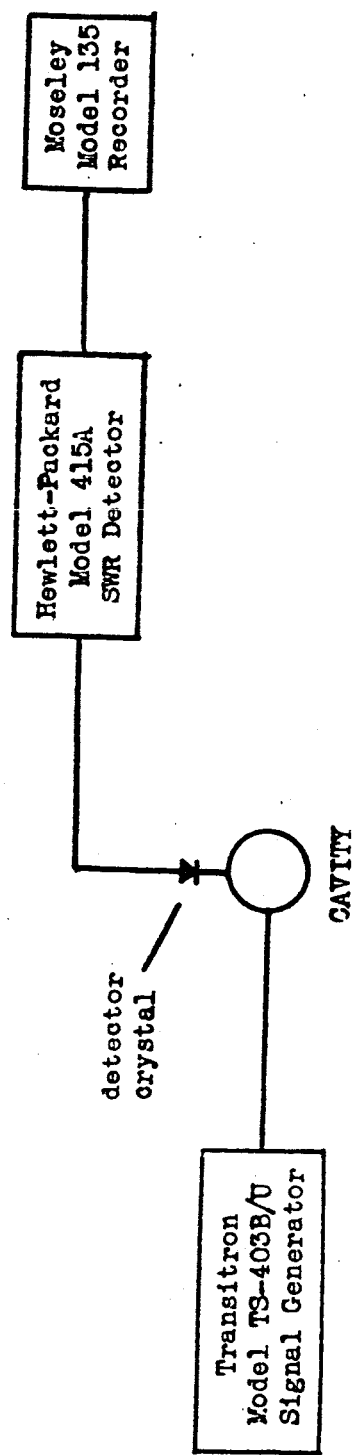


FIGURE 2. Block Diagram of Experimental Apparatus.

B. The Magnet

The cavity was mounted coaxially with an air-core magnet which was constructed of two large coils mounted in a Helmholtz-pair configuration (see Figure 3). The magnet coils were obtained from Harvey-Wells and were like those used on their Model L-128 Magnet. They measured 12" i.d., with a rectangular cross-section measuring 7.25" in the radial direction and 6" across. The coils were mounted in an upright position, each supported by a stand constructed out of aluminum (Figure 4). As can be seen from the figures, the stands were placed on tracks so that their position could be varied. Four spacers constructed as jack screws separated the two coils, and provided a continuous adjustment of the coil separation. A 1/2" aluminum plate with an eye in it could be inserted where the band surrounding the coils comes up into an eye, thus providing a means for lifting the coils safely with a crane. Brass and aluminum construction was used throughout.

Power was supplied to the coils by a Harvey-Wells Model HS-1050 magnet power supply, which has a current range of 0-50 DC amperes. Special connections for the coils were constructed of 3/8" i.d. copper tubing with heavy-duty, insulated welding cable inside. This provided a coaxial line to reduce distortion of the magnetic field of the air-core magnet by the field produced by external current-carrying conductors. The coils were connected in series by copper connectors inside a large switchbox which was provided to permit switching the power supply between this magnet and another one.

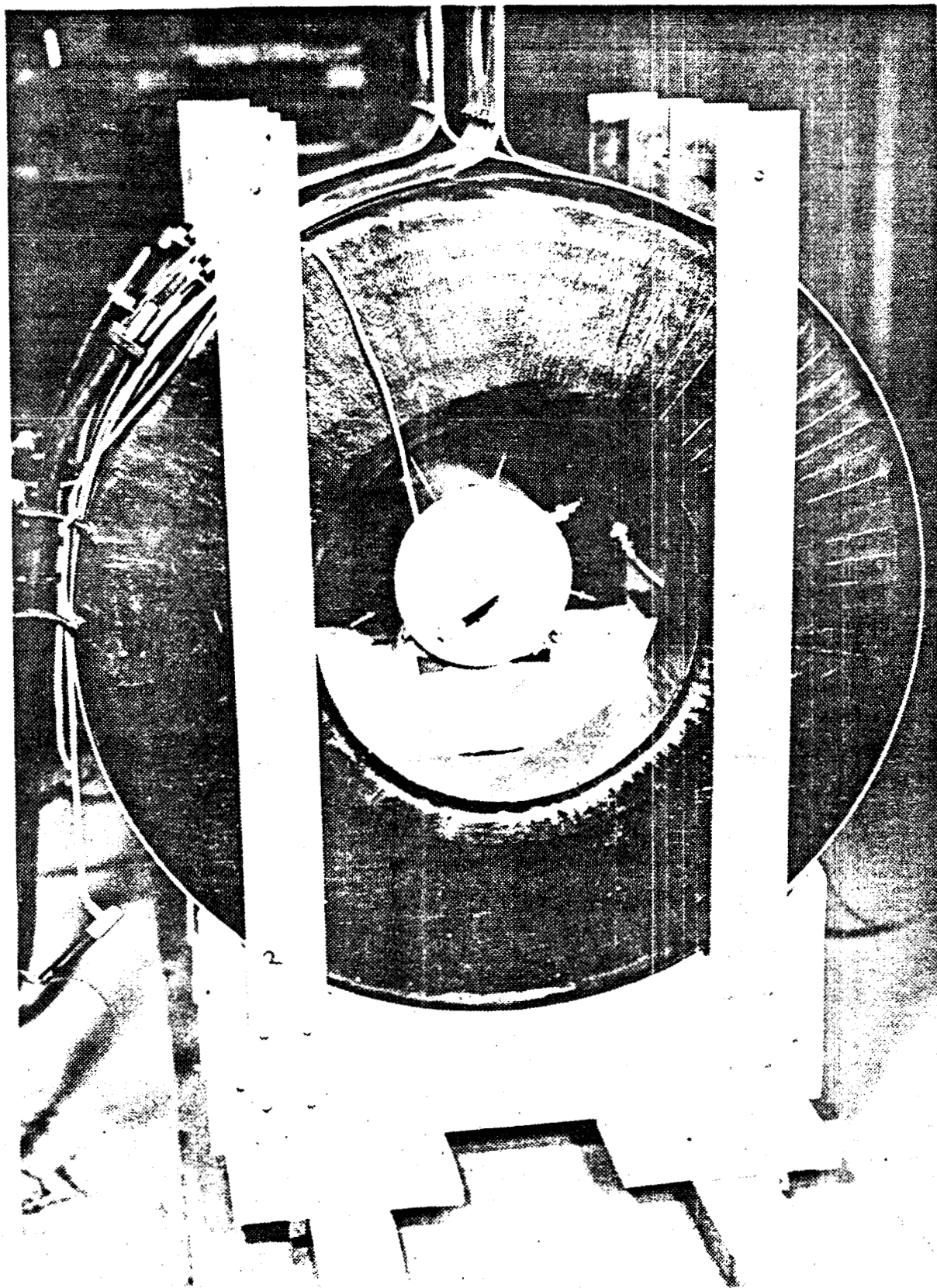


FIGURE 3. Photograph of Air-core Magnet and Cavity.

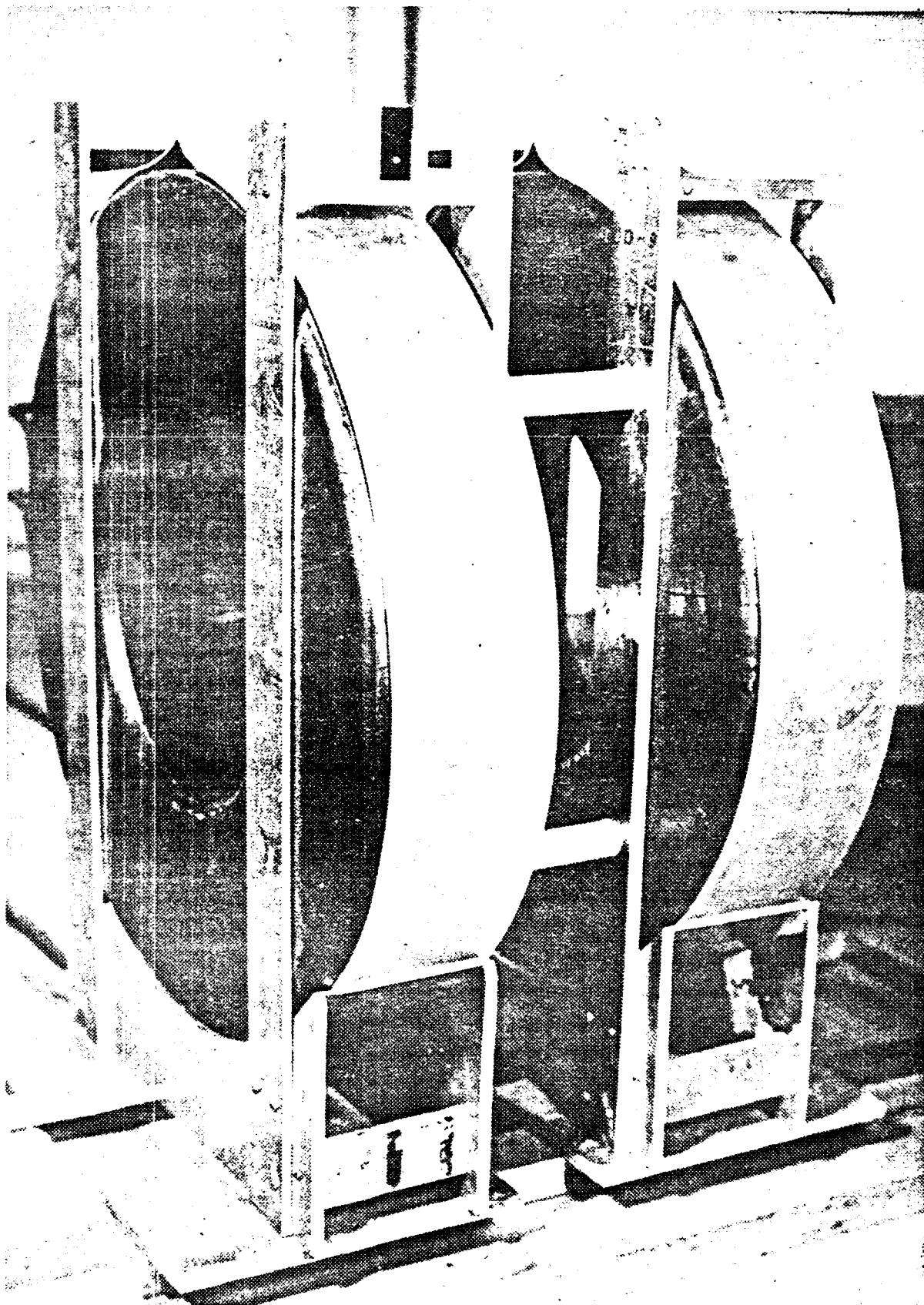


FIGURE 4. The Magnet.

The current-adjust control on the power supply was driven by a 4 RPM Holtzer-Cabot Motor. The motor was mounted in a 3" x 4" x 6" aluminum box and the box mounted on the panel over the control knob shaft. The shafts were connected by a short piece of Tygon tubing which fit snugly for non-slip turning, but which would give if the end point were reached before the motor was turned off. The box contained a power plug, a starting capacitor, an on-off switch, and a forward-reverse switch. The control required 10 turns for the complete range of 0-50 amps, so with this arrangement the current could be swept continuously in either direction in a period of 2.5 minutes. Since the magnet has an air-core, hysteresis is negligible and the field follows the current nicely.

In the experiment, the adjustable spacers were set to give a separation of 6" between the inside faces of the two coils. In this position, the maximum field was measured by the gaussmeter to be 1150 gauss. Calculations²⁴ were made using a digital computer which showed that the field along the coil axis should have less than 5% ripple, and measurements with the gaussmeter verified this result nicely.

C. The Cavity

A diagram of the cavity is shown in Figure 5. The cavity was bored from a solid, cylindrical piece of aluminum stock 5 1/2" long and 6" in diameter. The cylindrical cavity was 4.1" long by 5" in diameter.

²⁴ F. R. Crownfield, Jr. (to be published).

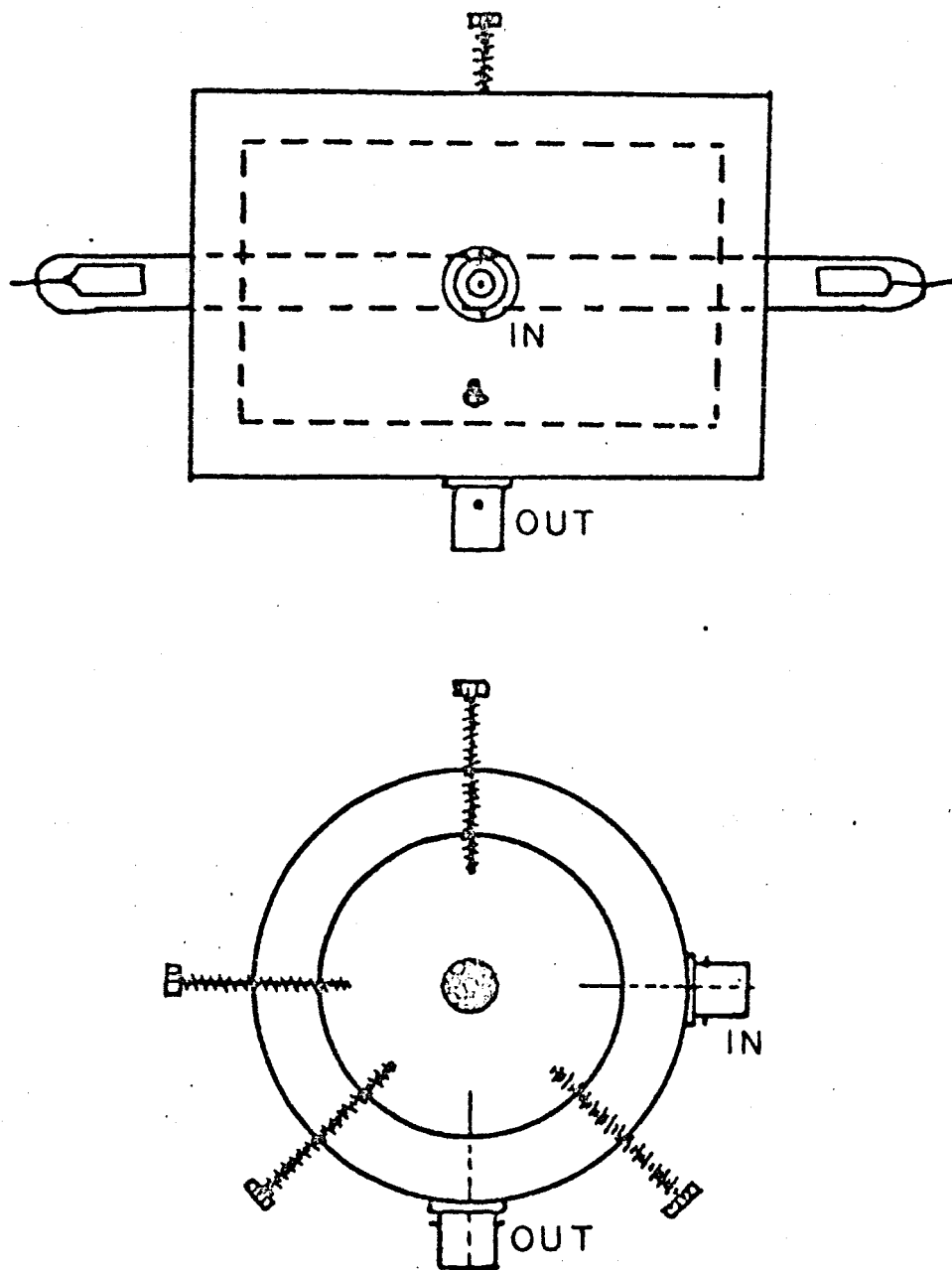


FIGURE 5. Diagram of microwave cavity.

The open end was closed by an aluminum end plate 1/2" thick, fastened with four 8-32 brass screws. A 37/64" hole was bored in the center of each end to accomodate the discharge tube.

The input and output antennas were placed in the mid-plane of the cavity at right angles to each other. Each of these was made by soldering a 1/4" piece of #22 AWG tin-coated copper wire into the tip of a BNC coaxial connector, which was screwed into a threaded hole in the cavity wall. Opposite each antenna was placed an 8-32 brass adjusting screw approximately 2" long. These served to tune the two cavity modes to the same frequency. Two similar screws were placed in the mid-plane at 45° either side of the input antenna to allow decoupling the modes. (All adjusting screws were provided with brass locknuts.)

D. The Discharge Apparatus

A total of four neon discharge tubes were used. The first was a straight tube with electrodes in each end, having an overall length of one foot and a diameter of 13 mm. The pressure of the neon in the tube was approximately 7.5 mm. of Hg. The other three tubes were similar, but with a length of one and a half feet and a diameter of 10 mm. These contained neon at separate pressures of 1 mm., 4 mm., and 10 mm. of Hg., as determined by a McLeod gauge. For each measurement, one of the tubes was mounted coaxially in the cavity as indicated above, with the electrodes projecting out of each end. It was connected in series with a power resistor (of sufficient value to give the desired current) to a power source.

The 1 mm. tube was operated from a 2800 volt transformer and a Variac while the others were operated by a Hewlett-Packard Model 711 A regulated DC power supply. The range of the power supply was 0-500 V. DC and 0-100 MA. DC.

IV. PROCEDURE AND DATA

The procedure was as follows: With the discharge tube placed in the cavity, artificial coupling between the input and output of the cavity was introduced by means of the coupling screws, so that the output signal would be small but large enough to detect easily. The signal generator was then tuned through the frequency range for which the cavity was calculated to be resonant for the TE_{111} mode. The resonant frequency would not be exactly that calculated for the empty, ideal cavity, since introduction of a dielectric such as the neon tube alters the resonant frequency. The resonant frequency was found when the meter on the output-signal amplifier suddenly indicated an output signal. The discharge was then turned on to a certain value of discharge current, which again produced a small shift in resonant frequency. The discharge also had the effect of destroying the microwave field in the cavity somewhat, so that when the signal generator was retuned to resonant frequency the peak of the output signal was not as large as before.

The tuning screws were then adjusted to give maximum symmetrical response to the detector as the signal generator was tuned either side of the maximum output. This served to tune the two modes to the same frequency. The coupling was then reduced and the tuning rechecked as before.

This procedure was followed until a null condition was reached, i.e., there was no power coupled to the output.

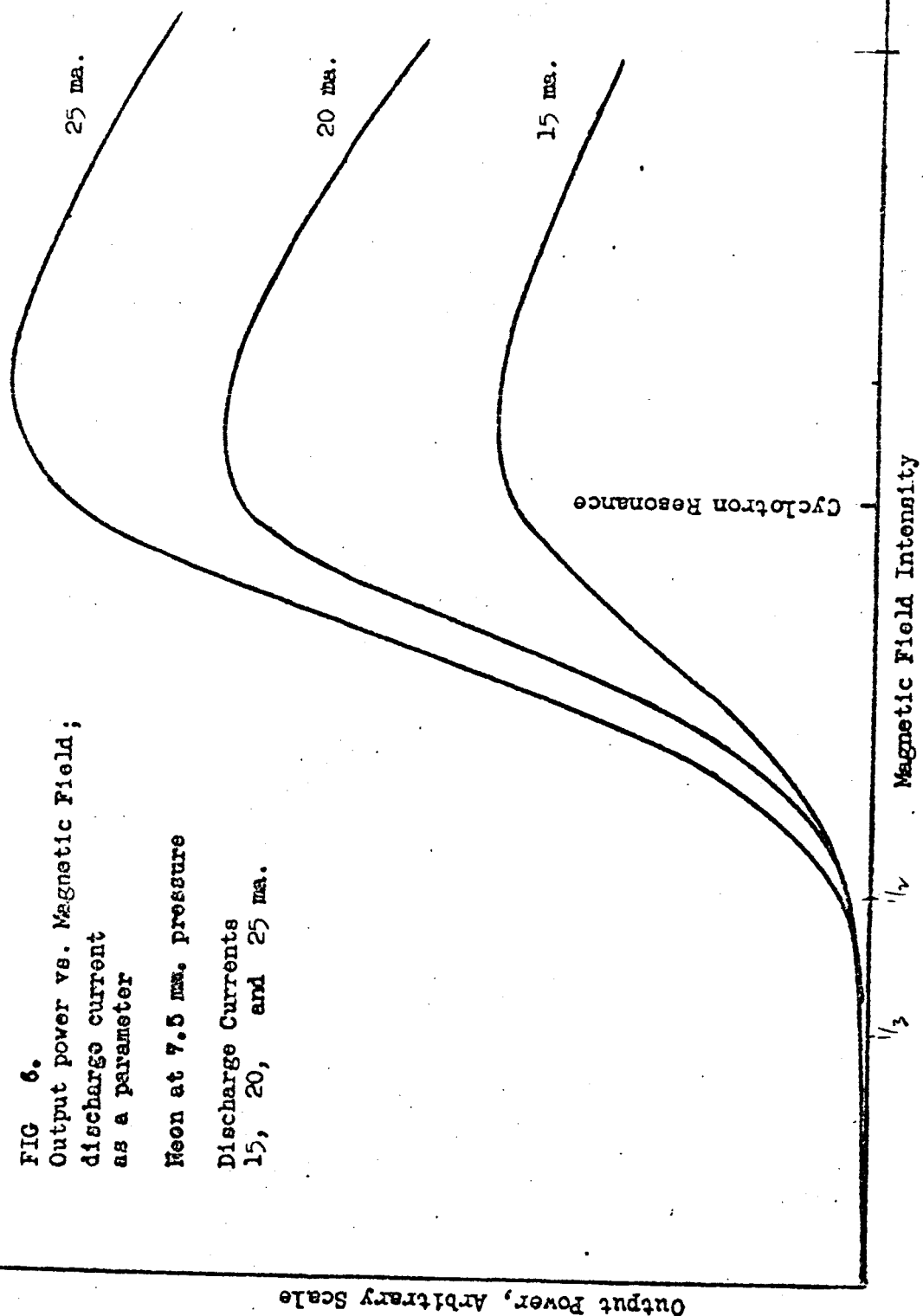
The Moseley Recorder was then zeroed properly on a standard-size piece of graph paper. The Y-range of the recorder was set so the cavity output signal would not drive the pen off scale, and the X-range either set on the internal time sweep at 20 seconds per inch or connected to the gaussmeter. The recorder and the magnet were then turned on; the magnetic field increased linearly with time because of the motor drive described previously. Both recorder and magnet were turned off when the maximum magnet current of 50 amps was reached. A check of the shift in the resonant frequency of the cavity at zero magnetic field, due to the discharge, showed the electron density to be approximately 10^9 to 10^{10} cm^{-3} for the discharge current used.

The initial runs were made with the 7.5 mm. pressure neon tube using a discharge current within the range of approximately 15-40 ma. For these runs the X-range of the recorder was operated on the time sweep, and the Y-range set at 2 MV. The SWR detector was set on the 50 db range. Due to imperfect functioning of the detector, the output signal was somewhat unsteady. An RC integrator was therefore employed on its output. This consisted of a .5 meg resistor and a 1 μ f capacitor, thus giving a half-second time constant. Typical results are shown in Figure 6 for three values of the discharge current. Coupled power is plotted against magnetic field. (The latter is a known function of time since the field increases linearly with time at a known rate.)

FIG 6.
Output power vs. Magnetic Field;
discharge current
as a parameter

Neon at 7.5 mm. pressure

Discharge Currents
15, 20, and 25 ma.



The value of the magnetic field could be obtained from the current reading on the magnet power supply, since the two are directly proportional; measurements with the gaussmeter gave the result as 23 gauss per amp of magnet current. The electron cyclotron frequency can be calculated from equation (6) written in the more convenient form

$$f_c = \frac{\omega_c}{2\pi} = 2.8 \text{ MC/gauss}$$

On these runs the resonant signal frequency was approximately 1942 MC. The magnetic field corresponding to cyclotron resonance at this frequency is indicated in Figure 6.

Figures 7a and 7b show recorder tracings when the 4 mm. and 10 mm. pressure tubes, respectively, were used. These were taken without the integrator, which allows the fluctuations from the SWR detector to appear, but which also allows observation of the relative change in the noisiness of the output signal from the cavity as a function of field. For these runs, the X-range of the recorder was operated by the gaussmeter, and was calibrated with the use of an 860 gauss standard calibrating magnet supplied with the gaussmeter. Figure 7a was taken with the SWR detector set on 50 db and the Y-range set on 20 MV. Figure 7b was similar but with the Y-range set on 2MV. The resonant frequency for both of these runs was 1986 MC, and cyclotron resonance as marked on the figures.

A recorder tracing of the low pressure (1 mm.) tube is shown in Figure 7c. As above, no integrator was used, but the SWR detector was set on the 40 db (less sensitive) range.

FIGURE 7a.
Output Power vs. Magnetic Field
Neon, 4mm. pressure
Discharge current: 12 ma.

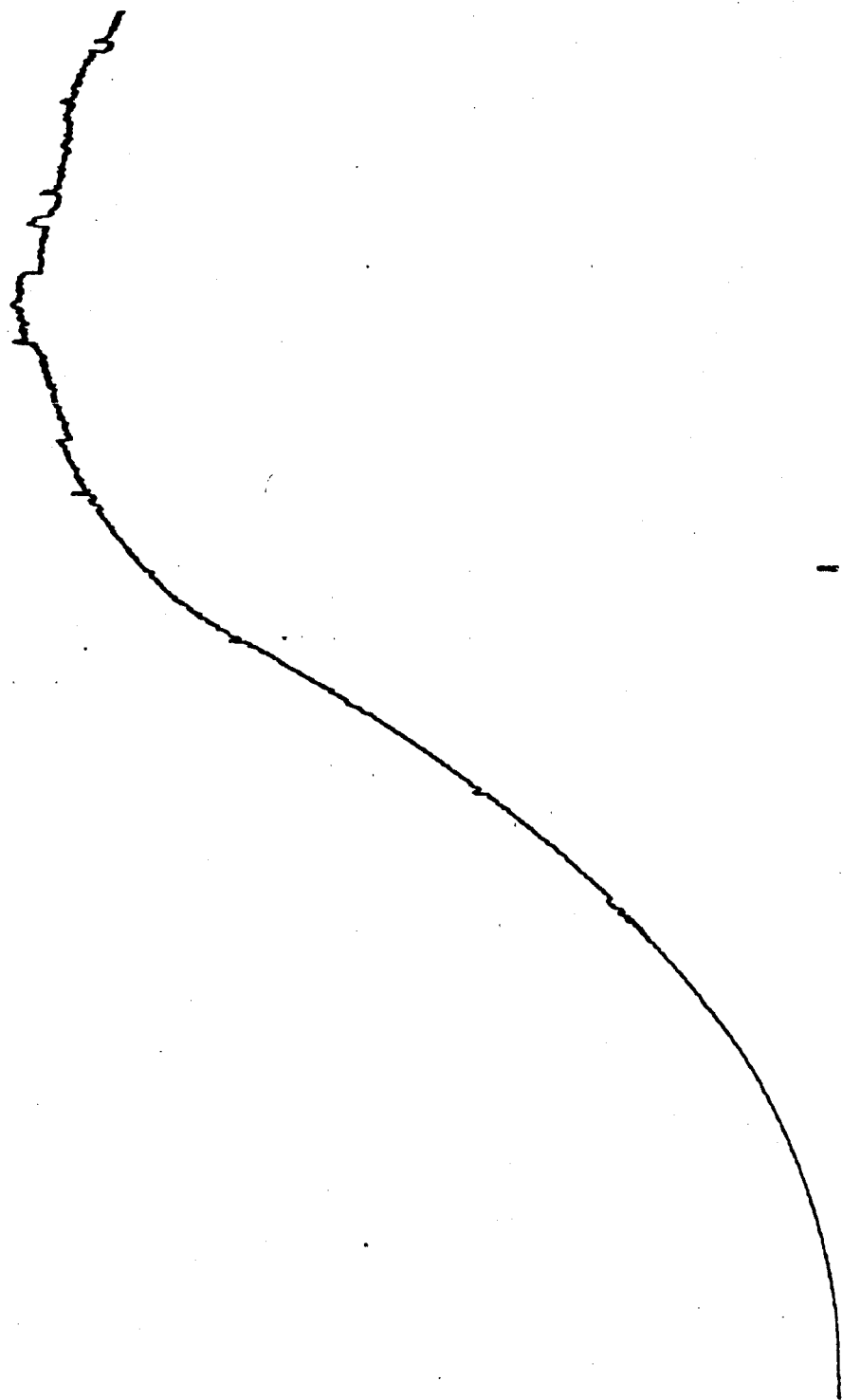


FIGURE 7b.
Output Power vs. Magnetic Field
Neon, 10 mm. pressure
Discharge current: 3 ma.

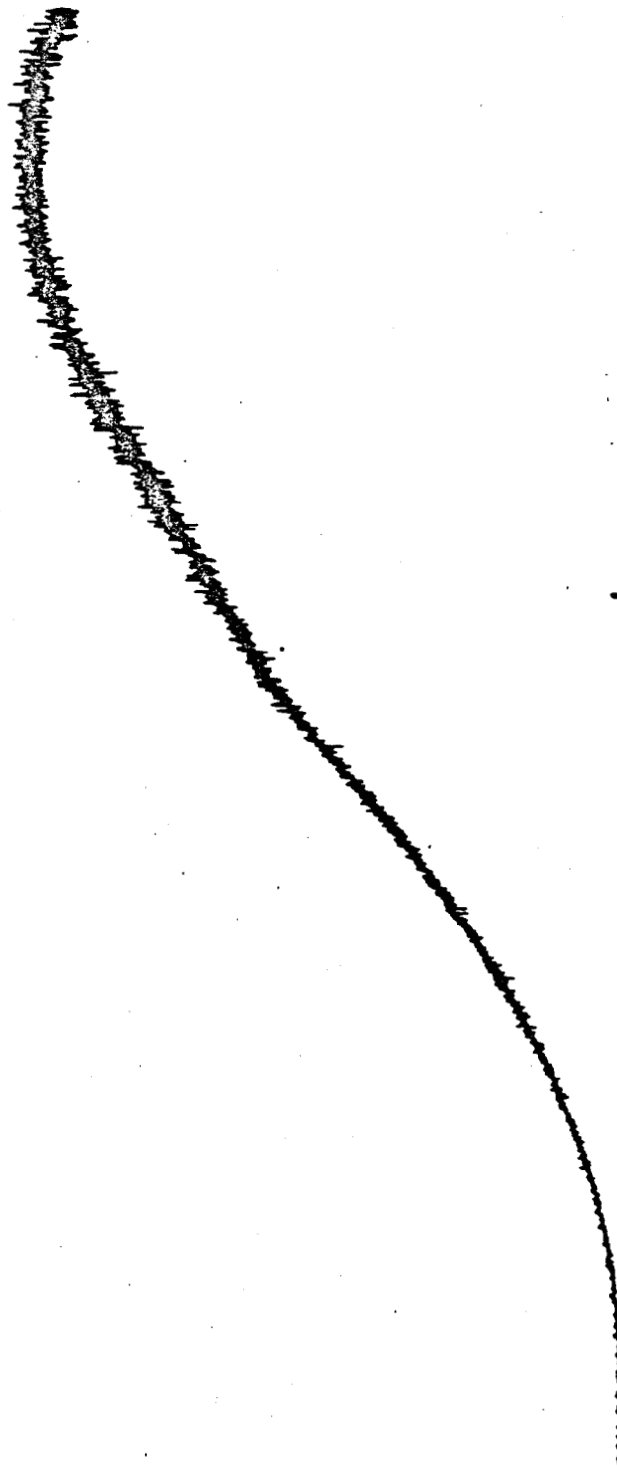
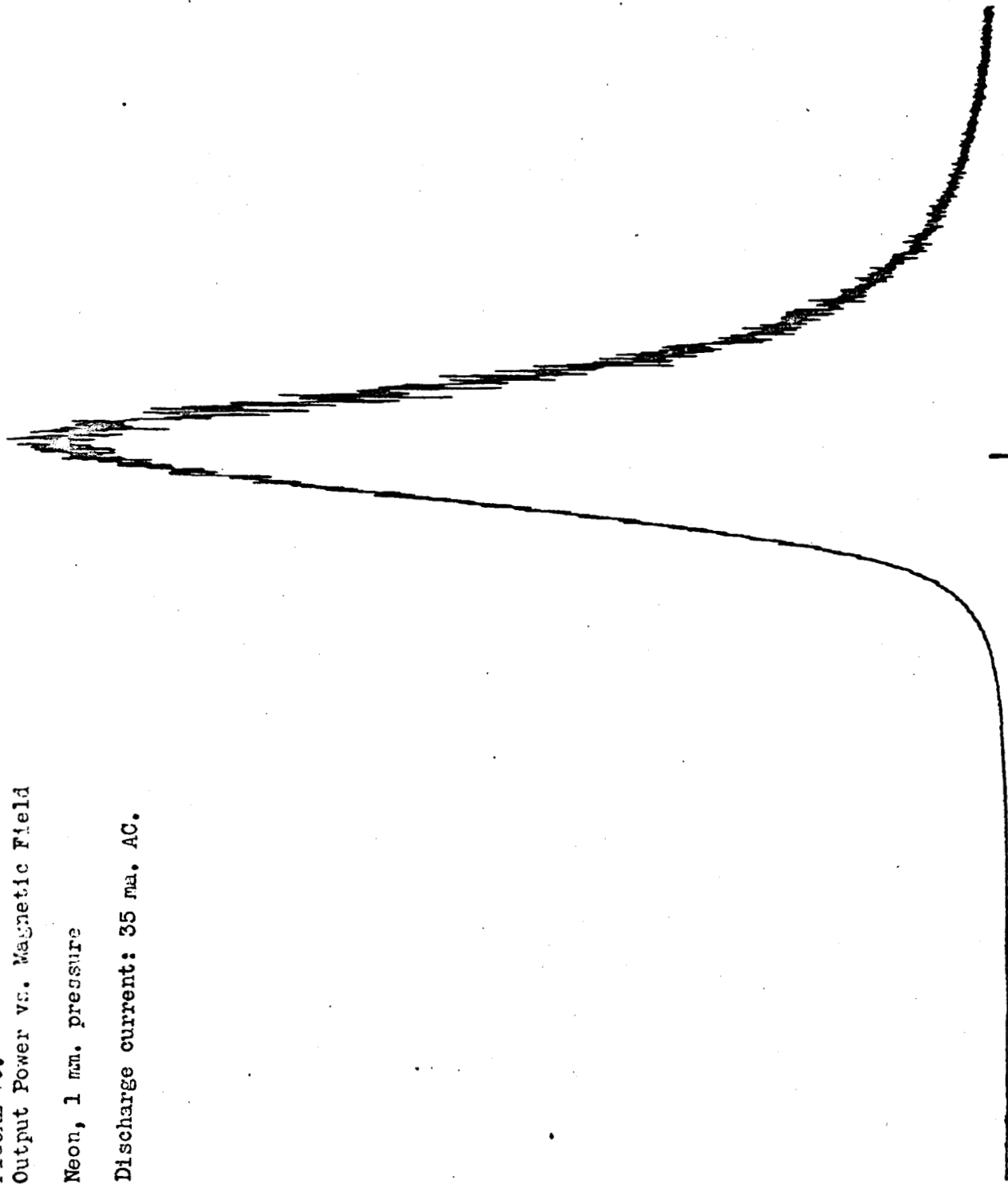


FIGURE 7c.
Output Power vs. Magnetic Field
Neon, 1 mm. pressure
Discharge current: 35 ma. AC.



The Y-range was set on 1 MV. and the X-range was operated by the time sweep as was used on the first tube. Resonant frequency was 1970 MC, and cyclotron resonance is marked in the figure. Additional runs could not be made with this tube because of the manner in which its characteristics changed in operation.

A calibration test of the receiving system indicated that it is approximately square law as expected, except for recorder deflections of less than perhaps 1/4 inch.

V. EXPERIMENTAL RESULTS AND CONCLUSIONS

The data given in the previous section seems to bear out the theory as presented in section II. For a given gas pressure (and hence collision frequency) the output power was approximately proportional to the square of the discharge current (or N^2), as seen from Figure 6. The most striking feature is the strong dependence of the resonance curve on the effective collision frequency, both experimentally and theoretically. The curves shown in the previous section behave in a manner similar to those of Figure 1 and as would be expected from equation (34). As seen in Figures 7a-c, the resonance peak is smeared out and to the right for higher pressures, while as the pressure becomes lower, the resonance becomes stronger, and sharper, and shifts to the left towards the magnetic field corresponding to cyclotron resonance. The curve for the 1 mm. tube shown in Figure 7c shows a nice sharp resonance peak just to the right of cyclotron resonance.

Although the above figures seem to show the expected dependence on collision frequency relative to each other, the effective collision frequencies seem to be somewhat higher than would be expected from their pressures. Using momentum transfer collision cross-sections and a pressure of 4 mm., one can estimate²⁵ the normalized collision frequency to be approximately $\frac{\nu}{\omega} = 0.068$.

²⁵J. Etter and L. Goldstein, U. of Illinois E. R. Res. Tech. Rept. No. 3, Contract No. AF19(604)-525, p. 59, 1954 (ASTIA No. AD53596).

However, comparison of the curve of the 4 mm. pressure tube shown in Figure 7a with Figure 1, a value of $\frac{\nu}{\omega}$ slightly above 0.55 would be inferred. In fact, equation (34) gives a value of $\frac{\nu}{\omega} = 0.566$. The reason for this discrepancy is not now understood and will be investigated further.

Because sealed-off tubes were used, their characteristics were not very stable with continued operation, making it difficult to repeat runs. This was especially true for low pressure tubes. It was also found that the apparent collision frequency often increased for low discharge currents. For high discharge currents (of the order of 50 ma.) it was not possible to take meaningful and reproducible data. (Possibly due to the changing characteristics of the tubes during operation).

Small bumps in the curve in the vicinity of harmonics of cyclotron resonance were sometimes observed, similar to absorption and radiation harmonics recently reported by Bekefi, et al.²⁶ However, they were not distinct or reproducible enough to be very convincing. It may be noted that the output signal becomes noisy in the vicinity of cyclotron resonance and beyond.

The investigation described herein is not complete in that it raised some questions as well as answered some. It was proposed to see if the bimodal-cavity technique provided a useful means for studying plasmas, and it is felt that this has been shown.

²⁶G. Bekefi, J. Coccoli, E. Hooper, Jr., and S. Buchsbaum, Phys. Rev. Letters 9, 6(1962).

It was possible to explain and observe Faraday Rotation in a magnetized plasma using this system. It proved to be quite sensitive, especially to the collision frequency of the plasma. In view of the strong dependence on collision frequency of the curves obtained, it is suggested that this method might provide a sensitive means for determining experimentally an effective electron collision frequency of a plasma. Present results, however, indicate that this effective collision frequency does not correspond to that determined from the electron-neutral momentum-transfer cross-section.

Further work is intended which will employ discharge tubes in which the gas pressure may be controlled by a vacuum pump. The ranges of pressure and discharge current will be extended. It is also planned to apply the method to other cavity modes, such as the TM_{112} , using a new cavity at a higher frequency. It is hoped that these and other extensions will help to answer some of the questions raised, and possibly allow measurements on cyclotron harmonics.

VI. SUMMARY

A survey of the background of the Faraday Effect and its measurement was given in order to afford a basic understanding of the problem. It was noted that previous measurements were done using the propagation method. Use of microwave cavities to study plasmas, and in particular a bimodal cavity to make spin resonance measurements, was cited. It was then proposed that the bimodal cavity technique be employed to study the Faraday Effect in magnetoplasmas.

Theory was presented which is based on the interpretation of the Faraday Effect in terms of a coupling between degenerate orthogonal modes of a cylindrical cavity containing a plasma in a magnetic field. This showed that the output signal was a resonance curve strongly affected by the collision frequency and also affected by the electron density of the plasma.

The experimental arrangement, discharge apparatus, the construction of the air-core magnet, and the bimodal cavity, were described.

Results were then presented which showed good qualitative agreement with the theory. The resonance curves obtained were smeared out to the right for higher pressures, while for lower pressures the resonance peak becomes strong, sharp, and approaches cyclotron resonance as a limiting value.

The effective collision frequency thus affects both the shape and magnitude of the resonance curves. The output power was observed to increase as the electron density was increased.

Harmonics of cyclotron resonance were not observed in the pressure and discharge current ranges studied, but it is planned to extend these ranges to study the possibility of the observation of cyclotron resonance harmonics.

BIBLIOGRAPHY

- Bekefi, G., Coccoli, J., Hooper, E., Jr., and Buchsbaum, S. J.,
Phys. Rev. Letters 9, 6 (1962).
- Berk, A. D. and Lax B., IRE Convention Record, Part 10, p. 65,
1953, (Also p. 70).
- Biondi, M. A., Rev. Sci. Inst. 22, 500 (1950).
- Buchsbaum, S. J., Mower, L., and Brown, S. C., Phys. Fluids 3 806 (1960).
- Drummond, J. D., Plasma Physics, (McGraw-Hill Book Company, Inc.,
New York 1961).
- Etter, J. E. and Goldstein, L., U. of Illinois E. E. Res. Tech. Rept.
No. 3, Contract No. AF 19(604)-525, 1954. (ASTIA No. AD 53596).
- Ginzburg, V. L., Propagation of Electromagnetic Waves in Plasma,
(Gordon and Breach Science Publishers, Inc., New York, 1961).
- Goldstein, L., Advances in Electronics and Electron Physics, Ed.
L. Marton, (Academic Press, Inc., New York, 1955), Vol. VII.
- Goldstein, L., Gilden, M., and Etter, J., IRE Convention Record
Part 10, p. 58, 1953.
- Goldstein, L., Lampert, M., and Heney, J., Phys. Rev. 82, 956 (1961).
- Huxley, L. G. H., Waveguides, (Macmillan Company, New York, 1947).
- Jenkins, F. A. and White, H. E., Fundamentals of Optics, (McGraw-
Hill Book Company, Inc., New York, 1957).
- MIT Radiation Laboratory Series, Ed. L. N. Ridenour, (McGraw-Hill
Book Company, Inc., New York, 1948), Vols. 6-11.
- Portis, A. M. and Teaney, D., J. Appl. Phys. 29, 1692 (1958).

Rao, K. and Goldstein, L., U. of Illinois E. E. Res. Sci. Rept. No. 3,
Contract No. AF 19(604)-3481, 1962. (ASTIA No. AD 276 736).

Rose, D. J. and Brown, S. C., J. Appl. Phys. 23, 1028 (1952).

Rose, D. J. and Clark, M., Jr., Plasmas and Controlled Fusion,
(The M.I.T. Press and John Wiley & Sons, Inc., New York, 1961).

Slater, J. C., Microwave Electronics, (D. Van Nostrand, Inc., Princeton,
N. J., 1950).

Suhl, H. and Walker, L. R., Bell Telephone Monograph No. 2322, 1954.

VITA

Maurice Terrell Raiford

Born in Franklin, Virginia, July 13, 1941. Attended Henry Clay High School, Ashland, Virginia, and graduated from Seabreeze High School, Daytona Beach, Florida, in 1957. Received the B.S. degree with honors from Guilford College, North Carolina, in June, 1961.

In September 1961, the author entered the College of William and Mary as a graduate student and research assistant in the Department of Physics.